

Infrared photodissociation of size-selected methylamine clusters

Udo Buck, Xijia Gu,^{a)} Reinhard Krohne, Christian Lauenstein,^{b)} Harold Linnartz,^{c)} and Andreas Rudolph

Max-Planck-Institut für Strömungsforschung, Bunsenstrasse 10, D 3400 Göttingen, Federal Republic of Germany

(Received 29 June 1990; accepted 5 September 1990)

Infrared photodissociation spectra of $(\text{CH}_3\text{NH}_2)_n$ clusters were measured from $n = 2$ to $n = 6$ near the absorption of the C–N stretching mode of the monomer at 1044 cm^{-1} using a line tunable cw CO_2 laser. The clusters are size selected by scattering them from a helium beam. The dimer spectrum shows a double-peak structure with a red- (1038 cm^{-1}) and a blue- (1048 cm^{-1}) shifted peak which is attributed to the nonequivalent position of the C–N in the open dimer structure. The larger clusters exhibit only one peak between 1045.4 and 1046.0 cm^{-1} which is caused by the equivalent position of the C–N in the cyclic structures of the larger clusters. Calculations of the minimum-energy configurations confirm these results. The linewidth increases by more than a factor of 3 for cold and internally excited dimers.

I. INTRODUCTION

There are not many methods to get direct information on the structure of molecular clusters. Most of them rely on spectroscopic results either from high-resolution vibrational-rotational spectra in the infrared¹ or from electronically excited states.² It takes special care to make sure that the correct cluster size is investigated. This is either provided by the spectrum itself or, for certain classes of molecules, by special detection methods like the two-color two-photon ionization near threshold in order to avoid fragmentation³ which is otherwise present. Very recently a promising new technique has been used to get this information, the Coulomb explosion of the cluster target by high-energy ion impact, and subsequent detection of the fragments.⁴ A different, more conventional method has been successfully used in this laboratory by combining the infrared photodissociation of weakly bound clusters⁵ with the size-selective process in a scattering experiment.⁶ The clusters which are generated in an adiabatic expansion are first size-selected by scattering them from a rare-gas beam and subsequently photodissociated. For that purpose a vibrational mode of one molecular component is excited by infrared laser photons. If the photon energy is larger than the binding energy of the cluster, the complex dissociates. The dissociation spectra are measured by the depletion of the beam signal, as a function of the laser frequency. From the measured line shift and linewidth of the excited molecular vibration detailed structural and dynamical information is obtained.^{7,8} The method has been applied to clusters up to $n = 8$ for the van der Waals systems C_2H_4 (Refs. 9–11) and SF_6 (Ref. 12) and the stronger bound molecules NH_3 (Ref. 13) and N_2H_4 (Ref. 14). Very recently the typical hydrogen-bonded methanol clusters have been investigated,^{15–17} where the photodissociation results agree well with an open dimer with a linear hydrogen bond, a cyclic

structure for the trimer, tetramer, and pentamer, and from the hexamer onwards with a heavily distorted structure which manifests itself in a spectrum with two splitted lines.

Methylamine has some similarities with methanol with a hydroxyl group being replaced by an amino group. The clusters can also be scattered into a reasonable large angle region for size selection because of its "light" mass. The CN stretch band of CH_3NH_2 at 1044 cm^{-1} is close to the CO stretch band of CH_3OH at 1033.5 cm^{-1} and both of them fall within the $9p$ branch of the CO_2 laser spectrum. The structures of isolated methylamine clusters have been calculated by Brink and Glasser¹⁸ using empirical potentials. They predicted that the most stable form of the dimer has an open structure and that the structure of the trimer and the tetramer has a cyclic structure in agreement with molecular-beam electric deflection experiments.¹⁹ Since there is no infrared spectroscopic information available for methylamine clusters, it is worthwhile to investigate the photodissociation of the size-selected CH_3NH_2 clusters in order to obtain some structural and energetic information.

In this article, we report such measurements with size-selected methylamine clusters. The spectral features vary from dimer to hexamer and are attributed to the different cluster configurations. Very small spectral shifts were observed for the trimer and higher clusters, a result which is different from that found for methanol.¹⁷

II. EXPERIMENT

A. Molecular-beam apparatus

The experimental apparatus consists of two crossed molecular beams which are together rotatable with respect to their scattering center and a fixed quadrupole mass spectrometer detector. In this detector the scattered particles are first ionized by electron impact, then mass selected in the quadrupole mass filter and finally counted by an electron multiplier. The velocity of the direct and scattered beams are measured by time-of-flight (TOF) analysis using a pseudo random chopper. A detailed description of the apparatus is given in Ref. 20. The actual beam data are presented in Table I. The $(\text{CH}_3\text{NH}_2)_n$ cluster beam is produced in

^{a)} Present address: Department of Chemistry, University of Toronto, Toronto, Canada M5S 1A1.

^{b)} Present address: Joint Institute for Laboratory Astrophysics, University of Colorado, Boulder, CO 80309.

^{c)} Permanent address: Department of Molecular and Laser Physics, Katholieke Universiteit Nijmegen, Toernooiveld, 6525 ED Nijmegen, The Netherlands.

TABLE I. Beam data.

	10% CH ₃ NH ₂ in He	0.1% CH ₃ NH ₂ in Ne	He
Nozzle diameter (μm)	80	60 ^a	30
Nozzle temperature (K)	300	300	300
Nozzle pressure (bars)	1.4	1.0	20
Peak velocity (m/s)	1404 ^b	819.2	1775
Speed ratio	27	28.9	70
Angular divergence (deg)	1.8	1.7	3.2
Collisional energy (meV)	94	...	

^a Conical nozzle (30°, length 1 mm).

^b Averaged peak velocity for all cluster sizes.

different mixtures with He and Ne. Very dilute mixtures favor the production of small clusters like dimers or trimers. In this experimental arrangement angular distributions with high velocity and angular resolution can be measured.

B. Laser system

For the photodissociation experiments, the scattered beam interacts collinearly with the radiation of a homemade continuous-wave CO₂ laser and the dissociation spectra are obtained by measuring the depletion of the signal as function of the laser frequency. A sketch of this arrangement is shown in Fig. 1. A detailed description of the apparatus can be found in Ref. 17. The CO₂ laser is a line-tunable flowing-gas laser. The resonator consists of a ZnSe output coupler, with a reflectivity of 85% and a curved grating of 150 lines/mm. For the dissociation of methylamine clusters the laser is operated at 10 W, which corresponds to a fluence of 42 mJ/cm².

III. RESULTS

A. Size selection

The size selection proceeds by the deflection of the cluster beam from the He beam. Figure 2 shows the kinematical (Newton) diagram calculated for the beam parameters of Table I. The velocities of all clusters are approximately the same as measured by the TOF spectrum. The limiting laboratory angles for the scattering of monomers to heptamers are given by 21.1°(1), 10.6°(2), 7.1°(3), 5.3°(4), 4.3°(5), 3.5°(6), and 3.0°(7). The numbers in parentheses are the corresponding cluster sizes. Each cluster size is confined to a specific angular range. If we set the detector, say, at 6°, clusters larger than $n = 3$ are excluded by these kinematical constraints. In order to exclude the smaller clusters $n = 1$ and

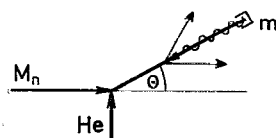


FIG. 1. Schematic view of the experimental setup. Both molecular beams, the cluster beam and the He beam, cross at an angle of 90° and can be rotated in such a way that the desired cluster size is scattered into the detector region where it interacts collinearly with the ir radiation of a homebuilt continuous wave CO₂ laser.

$n = 2$, a mass spectrometer can be used. This procedure, however, only works if the cluster $n = 3$ does not completely fragment during the ionization process to the next smaller cluster size. The information about this behavior can be obtained by measuring (1) the mass spectra with all fragment channels and (2) the angular distributions for these fragment channels. Figure 3 presents the mass spectrum of the (CH₃NH₂)_{*n*} clusters taken at 3° so that only cluster $n < 8$ contribute to the signals. The spectrum is, aside from the monomer fragments at 31 and 30 amu, completely dominated by the protonated species CH₃NH₃⁺ (CH₃NH₂)_{*n*-2} at $m = 32, 63, 94, 125, \text{ and } 156$ amu. The large peak at CH₃NH₃⁺ (32) already shows that fragmentation is appreciable for the clusters $n < 8$. This is confirmed by the measured angular distributions taken at the different fragment ion masses and shown in Fig. 4. The limiting angles for each cluster size are marked by arrows. A step in the angular dependence appears whenever a new cluster size contributes to the detection signal. At a deflection angle of 6° to which only clusters up to the trimer can contribute, we find signals of about 500 Hz at CH₃NH₂⁺, 700 Hz at CH₃NH₃⁺ and only 120 Hz at CH₃NH₃⁺ CH₃NH₂, the nominal protonated ion mass of the trimer. We conclude that in addition to the intra-cluster reaction

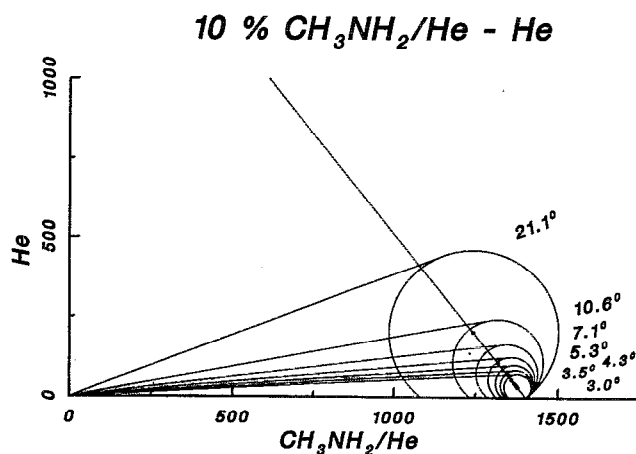


FIG. 2. The Newton diagram for the scattering of (CH₃NH₂)_{*n*} clusters seeded in He by He. The positions of elastically scattered clusters are drawn for $n = 1-7$ together with the listed limiting angles.

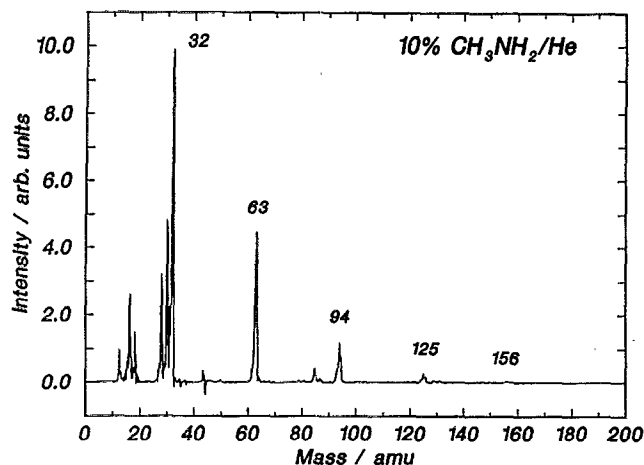
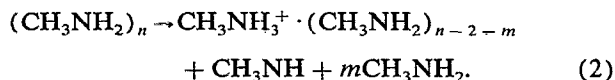


FIG. 3. The mass spectrum of a 10% $\text{CH}_3\text{NH}_2/\text{He}$ mixture at a scattering angle of 3° which contains all clusters $n < 8$. The indicated mass peaks correspond to $(\text{CH}_3\text{NH}_3)^+(\text{CH}_3\text{NH}_2)_{n-2}$ for $n = 2$ to $n = 6$.

which leads to the protonated species also further monomer units are lost according to the decay process



It occurs because the interaction of the CH_3NH_3^+ ion, formed after the first ionization step with the neutral partner molecule, leads to deeper well depths and smaller minimum distances²¹ compared with the neutral system, so that in a Franck-Condon-like transition the system is internally excited and a final probability exists that a neutral molecule evaporates. Compared with van der Waals or other systems (C_2H_4 , NH_3),^{22,23} the energetic differences are smaller for methylamine and there is always a small probability left to

TABLE II. Cluster composition of the different spectra.

No.	Θ (deg)	m (amu)	Fraction of cluster size n						
			2	3	4	5	6	7	8
1	8.5	32	1.0
2	6.0	63	...	0.90	0.10
3	5.0	94	0.70	0.25	0.05
4	4.0	125	0.60	0.30	0.10	...
5	3.0	156	0.50	0.30	0.20

detect a cluster $(\text{CH}_3\text{NH}_2)_n$ at its protonated ion mass $\text{CH}_3\text{NH}_3^+(\text{CH}_3\text{NH}_2)_{n-2}$ so that the size-selective process works well. The actual data for the photodissociation experiments are given in Table II. In contrast to what has been said before, the size selection is not pure. In all cases except for the dimer spectrum contributions from larger clusters cannot be ruled out, because of the finite angular resolution of the apparatus and the decreasing spacing of the limiting angles. These contributions are estimated from the measured angular distributions of the larger clusters.

B. Photodissociation

To analyze the measured data we apply a simple model based on one-photon absorption which leads to a dissociated fraction²⁴

$$P_{\text{diss}} = 1 - \exp[-L(\nu)] \quad (3)$$

with

$$L(\nu) = \sigma(\nu) \cdot F / (h\nu) \quad (4)$$

in which $\sigma(\nu)$ is the dissociation cross section, F the laser fluence (energy/area), and $h\nu$ the photon energy. If it is assumed that a photon is absorbed from the initial state i to the vibrationally excited state f and then directly coupled

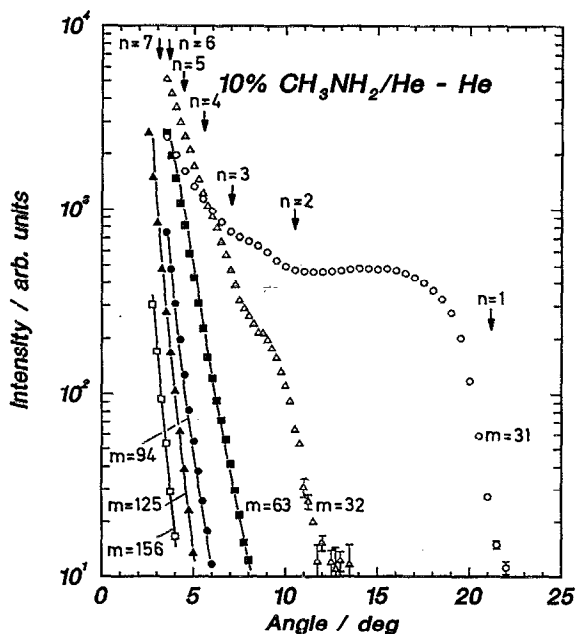


FIG. 4. The measured angular distribution of the scattered $(\text{CH}_3\text{NH}_2)_n$ clusters seeded in He at different detection masses. The onset of intensity at the limiting angles is marked by arrows.

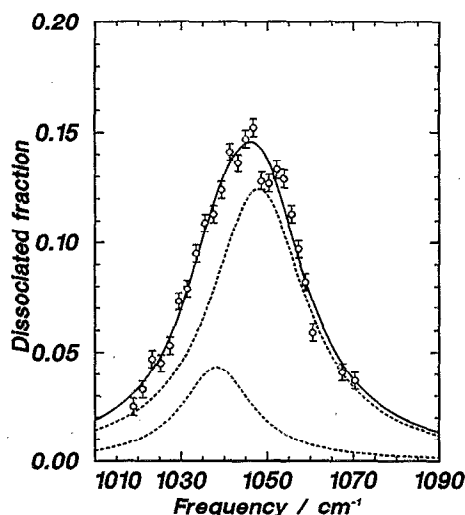


FIG. 5. The measured dimer dissociation spectrum for the 10% CH_3NH_2 mixture in He at a scattering angle of 8.5° . The dashed lines are the results of a fit using the position of the resolved measurement of Fig. 8(A).

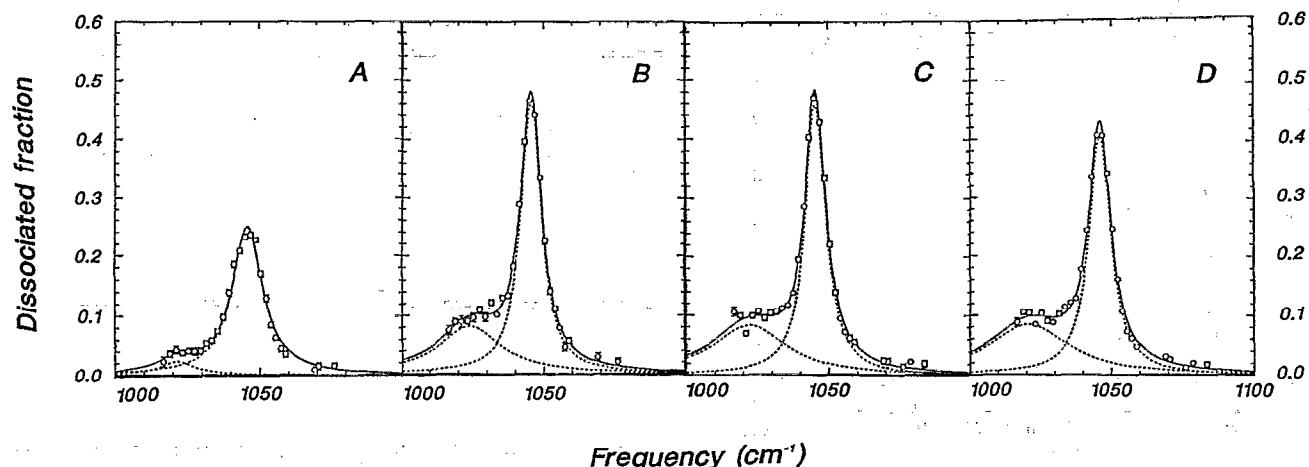


FIG. 6. The measured dissociation spectra for the clusters with $n = 3$ to $n = 6$ and the cluster composition of Table II. (A) is mainly the trimer spectrum at 6° ($m = 63$ amu), (B) the tetramer spectrum at 5° ($m = 94$ amu), (C) the pentamer spectrum at 4° ($m = 125$ amu), and (D) the hexamer spectrum at 3° ($m = 156$ amu).

to the continuum state α with energy E , the cross section is given by²⁵

$$\sigma(\nu, i \rightarrow \alpha E) = \frac{8\pi^2}{c} \nu |\langle i | \mu \mathbf{e} | f \rangle|^2 \frac{\Gamma}{(h\nu - h\nu_f)^2 + (\Gamma/2)^2}, \quad (5)$$

where μ is the transition dipole moment, \mathbf{e} the polarization vector, $h\nu_f$ the energy of the excited level, and Γ the dissociation rate, given by the golden rule expression

$$\Gamma = \pi |\langle f | V | \alpha E \rangle|^2 \quad (6)$$

with the intermolecular potential V for the coupling. Expression (3) is still valid, if more than one photon is absorbed provided the decay process is very fast.¹⁷ Therefore the data are evaluated by fitting Eq. (3) to the spectra. The function

$L(\nu)$ is a Lorentzian profile with the three free parameters ν_0 , the maximum frequency Γ , the full width at half maximum (FWHM), and L_0 , the value of the maximum. It is noted that the cross section, integrated over the Lorentzian profile, is proportional to $L_0\Gamma$. If the spectrum for one cluster size is given by two or more profiles a sum of the corresponding Lorentzians is used in Eq. (3).

In the spectral region of the CN stretching mode (ν_8) of methylamine, the photodissociation spectra are measured by varying the CO_2 -laser lines at constant power for different cluster sizes using the conditions of Table II. The results obtained at a laser fluence of 42 mJ/cm^2 are shown in Figs. 5 and 6. The parameters for the Lorentzian line shapes are presented in Table III. All the spectra exhibit a large maximum between 1045.4 and 1046.0 cm^{-1} slightly shifted to the

TABLE III. Parameters of the fitted Lorentzian curves for the different clusters.

A. Scattered beam: 10% CH_3NH_2 in He-He									
No. ^a	n	Fig.	C-N stretch				Broad peak		
			ν_0 (cm^{-1})	Γ (cm^{-1})	L_0	$L_0\Gamma$	ν_0 (cm^{-1})	Γ (cm^{-1})	L_0
1	2	5	1038.3	19.8	0.04	0.87
			1047.9	26.3	0.13	3.49			
2	3	6(A)	1045.8	11.3	0.248	2.8	1020.5	16.3	0.024
3	4	6(B)	1045.5	6.3	0.456	2.9	1024.5	25.2	0.082
4	5	6(C)	1045.4	6.2	0.459	2.9	1022.1	30.1	0.085
5	6	6(D)	1046.0	7.1	0.403	2.9	1021.0	32.0	0.085
B. Direct beam: 0.1% CH_3NH_2 in Ne									
n	Fig.	C-N stretch				Broad peak			
		ν_0 (cm^{-1})	Γ (cm^{-1})	L_0	$L_0\Gamma$	ν_0 (cm^{-1})	Γ (cm^{-1})	L_0	
2	8(A)	1038.3	8.5	0.030	0.26	
		1047.9	8.1	0.050	0.42				
2	8(B)	1038.8	4.7	0.029	0.14	1032.0	15.0	0.15	
		1047.9	8.0	0.057	0.45				
3	7	1046.1	6.1	0.52	3.19	1028.0	20.9	0.048	

^a From Table II.

blue from the gas-phase frequency of the CN stretch at 1044 cm^{-1} .²⁶ The halfwidth decreases dramatically from more than 20 cm^{-1} for the dimer and 11.3 cm^{-1} for the trimer to about 6 cm^{-1} for the larger clusters. From the trimer to the hexamer there also exists a smaller peak at the lower-frequency side around $1020\text{--}1025 \text{ cm}^{-1}$. The only frequency reported in literature in this frequency range is the overtone excitation of $2\nu_{15}$, the NH_2 torsion, which has been observed in the spectrum of the solid near 1005 cm^{-1} .²⁶

While the existence of one large peak of the CN stretch mode is very pronounced for all spectra from the trimer to the hexamer, the same conclusion is somewhat doubtful for the dimer. There seems to be some structure in the spectrum which can be attributed to a peak splitting around 1042.5 and 1054 cm^{-1} . A better resolution of any line splitting is hindered by the relative large linewidth of the spectrum. Since this is essentially caused by the internal excitation of the dimer during the scattering process with helium, we have repeated the dimer measurement with cold species without scattering in a direct beam experiment of CH_3NH_2 seeded in Ne. The beam data are given in Table I. In order to get size selectivity very diluted mixtures of CH_3NH_2 in Ne were used in this experiment. Results are shown in Figs. 7 and 8 for two different masses. If the spectrometer is tuned to $m = 63$ amu, only trimers and heavier clusters are detected. For the 0.32% mixture one large peak appears, of which the maximum position agrees well with the results of the size-selected experiment (Fig. 7). For the 0.1% mixture the peak completely disappears, thus indicating that the beam is free of higher clusters than the dimer. For this mixture and a mass of $m = 33$ amu, the pure dimer spectrum is measured. A clear line splitting is observed with the line positions at 1038 and 1048 cm^{-1} [Fig. 8(A)]. The fit gets even better if a very small peak around 1030 cm^{-1} is added which can again be attributed to an overtone excitation of the $2\nu_{15}$ torsion [Fig. 8(B)]. If we use the values obtained in the fitting procedure of Fig. 8(A) for the size-selected internally excited dimer, a satisfactory fit is obtained as is demonstrated in Fig. 5. Thus

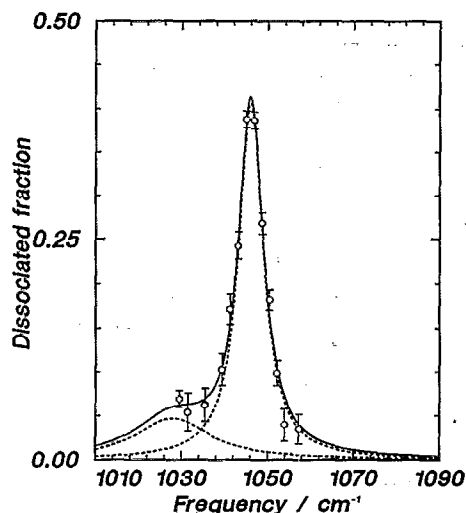


FIG. 7. The trimer dissociation spectrum for the 0.32% CH_3NH_2 mixture in Ne measured at $m = 63$ amu in the direct beam.

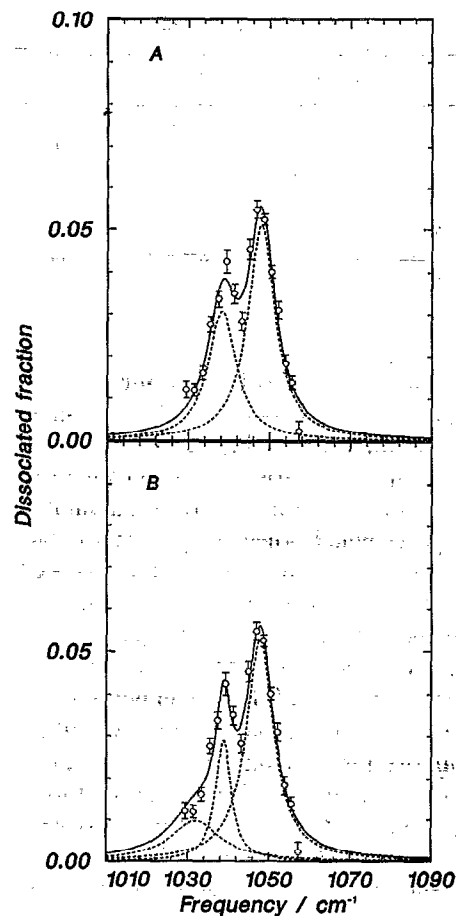


FIG. 8. The dimer dissociation spectrum for the diluted 0.1% CH_3NH_2 mixture in Ne, measured in a direct beam experiment. A clear double-peak structure is found (A). In (B) a small contribution around 1030 cm^{-1} is added in the fit which is also seen for the larger clusters.

we conclude that the dimer displays a line splitting for the excitation of the ν_8 mode of 10 cm^{-1} between 1038 and 1048 cm^{-1} .

IV. DISCUSSION

A. Line shifts and structure implications

One of the first aspects to notice is the complete change of line profile for the transition from the dimer to the trimer spectrum. For the trimer and the larger clusters, there is one dominating maximum at $1045.5 \pm 0.5 \text{ cm}^{-1}$ which is caused by the excitation of the C-N stretching mode. The smaller shoulder around 1020 cm^{-1} results probably from the $2\nu_{15}$ torsion. For the dimer, however, there are two distinct maxima, one (shifted to the red) at 1038 cm^{-1} and one (shifted to the blue) at 1048 cm^{-1} . There is a clear line splitting for the excitation of the ν_8 mode of about 10 cm^{-1} . Furthermore, it is also possible to fit the contribution of the $2\nu_{15}$ torsion into the dimer spectrum. This does not change the structure of this spectrum. Therefore it is very likely that the line splitting of the dimer and the single line of the larger clusters are originating from different cluster structures.

A more detailed understanding of the observed dissociation spectra can be achieved, if one looks at the calculated minimum configurations for the methylamine clusters. The

TABLE IV. Total energy of the most stable cluster configurations in kJ mol^{-1} .

Cluster size	This work	Ref. 18	ΔE^a	Configuration
$n = 2$	-13.38	-13.64	13.4	open
$n = 3$	-37.24	-37.55	23.9	cyclic
$n = 4$	-60.10	-59.97	22.9	cyclic
$n = 5$	-89.80	...	29.7	cyclic
$n = 6$	-117.81	...	28.0	cyclic, distorted

^a Energy necessary to remove one monomer.

configurations are calculated by the EPEN/2 (empirical potential of electrons and nuclei) model.²⁷ To find the most likely configuration one molecule is fixed and the coordinates of the other molecules are varied to find a configuration with minimum energy. The results for the total binding energies and the energy ΔE which is necessary to remove one monomer are given in Table IV. The results agree very well with similar calculations carried out up to the tetramer.¹⁸ The dimer prefers an open configuration, while greater clusters have cyclic structure which start to get distorted for $n = 6$. If one regards the influence of the cluster bond on the excited CN stretch, it becomes clear that there are two different possibilities within the dimer. In one molecule the nitrogen atom is bound within the cluster, while in the other molecule the N atom just sees a slightly different bond with respect to a hydrogen atom, but does not participate in the cluster bond. In the cyclic configurations of the greater clusters all CN bonds are disturbed in the same way. In these configurations all N atoms contribute to the cluster bond and at the same time all of them have a H-atom bond, which is changed by the cluster bond in the same way.

The absorption frequencies for the CN stretching mode of gaseous (1044 cm^{-1}) and solid (1048 cm^{-1}) methylamine are very close together. The maxima of the greater clusters lie exactly between these two values. The measured absorption of isolated molecules in a matrix also shows an interesting splitting in the stretching mode of 1041 and 1051 cm^{-1} . In Ref. 28 this is explained by the different positions, which the molecules have in the matrix or by polymerized molecule bonds. Compared with the positions found for the dimer splitting, these matrix values are just 3 cm^{-1} shifted to the blue, which supports the idea of two differently bound N atoms in the methylamine dimer.

If we compare these measurements with the results for methanol¹⁷ we see that both dimers exhibit a similar splitting due to the same effect. The splitting, however, is smaller in the present case. For the higher clusters the similarity continues concerning the one-peak structure, but for CH_3NH_2 the maximum does not shift with increasing cluster size and the shift with respect to the gas absorption frequency is much less. Furthermore, we see no line splitting for the $(\text{CH}_3\text{NH}_2)_6$ cluster, as was found for the methanol hexamer. However, the linewidth is slightly broader than in the case of the smaller cyclic clusters. Since for $(\text{CH}_3\text{NH}_2)_n$ clusters line shifts are generally smaller than for CH_3OH , it can be assumed that a small line splitting is present which is not resolved in the present experiment. The alternative explanation that $(\text{CH}_3\text{NH}_2)_6$ exhibits a well-behaved cyclic

structure which, in contrast to $(\text{CH}_3\text{OH})_6$, is not very much distorted is less probable. Such a structure is not found in the calculations.

B. Linewidth

The linewidth is strongly influenced by the amount of energy transferred into the cluster by the scattering process. This is clearly seen for the dimer, if we compare the results for the scattered and the direct beam. The Γ values are 19.8 and 26.3 cm^{-1} for the internally excited dimers and 8.5 and 8.1 cm^{-1} for the cold dimers. The effect for the trimer is smaller (11.3 cm^{-1} vs 6.1 cm^{-1}). With increasing clusters size the broadening effects decrease, probably because the transferred energy can be better distributed among the more degrees of freedom.

While the differences in the linewidth between the scattered and the direct beam can be traced back to the internal excitation in the scattering process, we are left with the intrinsic linewidth of about 8 cm^{-1} for the cold dimer. The interpretation of this number is difficult. The line tunability of the laser and the resulting low resolution does not allow interpretation of the linewidth as homogeneously broadened, so that very probably a contour of an unresolved band is measured which contains contributions of rotation and internal rotations as well as the predissociation lifetime. It is interesting to note that the value found here for CH_3NH_2 dimers is larger than the result for CH_3OH dimers under similar experimental conditions, for which values smaller than 3 cm^{-1} have been reported.²⁹ The reason is probably the additional internal rotation of the NH_2 group in combination with or without a faster decay caused by the additionally accessible vibrational band of the NH_2 -wagging mode at 780 cm^{-1} . This band is relatively close to the originally excited band and should according to the momentum gap law enhance the predissociation rate.⁵

C. Cross sections

The L_0 values listed in Table III are directly proportional to the cross sections at the maximum σ_0 . The calibration constant is according to Eq. (3) and the known values of the fluence and frequency $0.5 \times 10^{-18} \text{ cm}^2$. These values increase with increasing cluster size up to $n = 4$ and then level off. What, however, is really important for the absorption process is the average transition dipole moment which according to Eq. (5) is proportional to ΓL_0 . These values are also listed in Table III. For the dimer we find, if the two components are added, a large difference between the values of the internally excited (4.36) and the cold (0.68) species.

For the larger clusters a nearly constant value of 2.9 is found. Both results are at variance with what would be expected for the absorption cross sections. For one cluster species, the dimer, it should be constant, and for larger clusters it should increase linearly with the number of absorbers, a result which is indeed found for $(\text{C}_2\text{H}_4)_n$ clusters.³⁰ The reason for the deviations from the expected behavior can be found, if we look at the bonding energies and the number of absorbed photons. For the dimer a bonding energy of 13.4 kJ/mol is calculated, while the laser photon corresponds to 12.5 kJ/mol. Even if a certain amount of zero-point energy is accounted for in addition to the uncertainty of the calculated numbers, it is obvious that a cold cluster can be dissociated only by two photons, while an internally excited cluster with an additional energy of about 3 kJ/mol is dissociated by one photon. This result probably explains the large difference in the absorption cross section.

Similar considerations hold for the larger clusters. There are two contradicting influences for these species. The cross section should increase with an increasing number of absorbers, and it should decrease with an increasing bonding energy and the increasing number of photons necessary to break these bonds. This is clearly seen in the results of Table IV which require, at least, two photons for $n = 3$ and $n = 4$ and three photons for $n = 5$ and $n = 6$. These arguments explain the nearly constant behavior of the cross section.

ACKNOWLEDGMENTS

We gratefully acknowledge the financial support from the Deutsche Forschungsgemeinschaft (SFB 93). We thank B. Schmidt for carrying out the calculation of the minimum-energy configurations of the $(\text{CH}_3\text{NH}_2)_n$ clusters for $n = 5$ and $n = 6$.

¹R. E. Miller, *Science* **240**, 447 (1988).

²S. Leutwyler and J. Jortner, *J. Phys. Chem.* **91**, 5558 (1987).

³U. Buck, *J. Phys. Chem.* **92**, 1023 (1988).

⁴Z. Vager, R. Naaman, and E. P. Kanter, *Science* **244**, 426 (1989).

⁵R. E. Miller, *J. Phys. Chem.* **90**, 330 (1986).

⁶U. Buck and H. Meyer, *Phys. Rev. Lett.* **52**, 109 (1984); *J. Chem. Phys.* **84**, 4854 (1986).

⁷U. Buck, in *Enrico Fermi School on the Chemical Physics of Atomic and Molecular Clusters*, edited by G. Scoles (Il Nuovo Cimento, Bologna, 1990).

⁸U. Buck, X. J. Gu, M. Hobein, Ch. Lauenstein, and A. Rudolph, *J. Chem. Soc. Faraday Trans. II*, 1923 (1990).

⁹F. Huisken, H. Meyer, Ch. Lauenstein, R. Sroka, and U. Buck, *J. Chem. Phys.* **84**, 1042 (1986).

¹⁰F. Huisken and T. Pertsch, *J. Chem. Phys.* **86**, 106 (1987).

¹¹U. Buck, F. Huisken, Ch. Lauenstein, H. Meyer, and R. Sroka, *J. Chem. Phys.* **87**, 6276 (1987).

¹²F. Huisken and M. Stemmler, *Chem. Phys.* **132**, 351 (1989).

¹³F. Huisken and T. Pertsch, *Chem. Phys.* **126**, 213 (1988).

¹⁴U. Buck, X. J. Gu, M. Hobein, and Ch. Lauenstein, *Chem. Phys. Lett.* **163**, 455 (1989).

¹⁵U. Buck, X. J. Gu, Ch. Lauenstein, and A. Rudolph, *J. Phys. Chem.* **92**, 5561 (1988).

¹⁶F. Huisken and M. Stemmler, *Chem. Phys. Lett.* **144**, 391 (1988).

¹⁷U. Buck, X. J. Gu, Ch. Lauenstein, and A. Rudolph, *J. Chem. Phys.* **92**, 6017 (1990).

¹⁸G. Brink and L. Glasser, *J. Mol. Struct.* **85**, 317 (1981).

¹⁹J. A. Odutola, R. Viswanathan, and T. R. Dyke, *J. Am. Chem. Soc.* **101**, 4787 (1979).

²⁰U. Buck, F. Huisken, J. Schleusener, and J. Schäfer, *J. Chem. Phys.* **72**, 1512 (1980).

²¹S. S. Wee, S. Kim, M. S. Ihon, and H. A. Scheraga, *J. Phys. Chem.* **94**, 1656 (1990).

²²U. Buck, Ch. Lauenstein, H. Meyer, and R. Sroka, *J. Phys. Chem.* **92**, 1916 (1988).

²³U. Buck and Ch. Lauenstein, *J. Chem. Phys.* **92**, 4250 (1990).

²⁴M. P. Cassasa, D. S. Bomse, and K. C. Janda, *J. Chem. Phys.* **74**, 5044 (1981); M. A. Hoffbauer, K. Liu, C. F. Giese, and W. R. Gentry, *ibid.* **78**, 5567 (1983).

²⁵J. A. Beswick, in *Structure and Dynamics of Weakly Bound Molecular Complexes*, edited by A. Weber (Reidel, Dordrecht, 1987), p. 563.

²⁶J. R. Durig, S. F. Bush, and F. G. Baglin, *J. Chem. Phys.* **49**, 2106 (1968).

²⁷J. Snir, R. A. Nemenoff, and H. A. Scheraga, *J. Chem. Phys.* **82**, 2497 (1978); L. L. Shipman, A. W. Burgess, and H. A. Scheraga, *Proc. Natl. Acad. Sci. U.S.A.* **72**, 543 (1975).

²⁸G. C. Pimentel, M. O. Bulanin, and M. van Theil, *J. Chem. Phys.* **36**, 500 (1965).

²⁹J. P. LaCosse and J. M. Lisy, *J. Phys. Chem.* **94**, 4398 (1990).

³⁰R. Ahlrichs, S. Brode, U. Buck, M. De Kieviet, Ch. Lauenstein, A. Rudolph, and B. Schmidt, *Z. Phys. D* **15**, 341 (1990).